Eur. Phys. J. C (2024) 84:411
https://doi.org/10.1140/epjc/s10052-024-12761-2

THE EUROPEAN PHYSICAL JOURNAL C

Regular Article - Theoretical Physics

Photon scattering by an electric field in noncommutative spacetime

Daniela D'Ascanio[a], **Pablo Pisani**[b], **Ulises Wainstein Haimovichi**[c]

Instituto de Física La Plata (IFLP; UNLP-CONICET), La Plata, Argentina

Received: 31 January 2024 / Accepted: 4 April 2024 / Published online: 22 April 2024

Abstract As is known, the existence of a small noncommutativity between coordinates would generate nonlocal self-interactions in the electromagnetic theory. To explore some consequences of this effect on the propagation of photons we consider Moyal space half-filled with a static and homogeneous electric field and analyze electromagnetic fluctuations on top of this step-like background. Both the localization of photons and the possibility of photon production by strong electric fields are addressed. Several aspects of the Klein paradox in this setup are discussed as well.

Contents

1 Introduction

As a rule, photons do not interact among themselves. Nevertheless, such self-interaction is possible in noncommutative (NC) spacetimes. Moyal spacetime is a most natural NC scenario where noncommutativity between coordinates can be represented by the Moyal $\star$-product between fields [1,2]. Electrodynamics in this spacetime, known as $U(1)_\star$, has been extensively studied: as a first remarkable feature one finds that noncommutativity introduces nonlinearities in Maxwell's equations through a self-interaction which is nonlocal already at the classical level. In other words, since gauge fields – as functions of NC coordinates – do not commute, $U(1)_\star$ holds a close resemblance with nonabelian Yang–Mills theories (see the recent lecture notes [3]).

The goal of the present work is to expose some aspects of this self-interaction in the scattering of photons by a static electric field background. One of our original motivations was the question of whether noncommutativity allows photon creation by intense electromagnetic fields (the effects of noncommutativity on electron/positron production by strong electric fields can be found in [4]). Although the answer requires a quantum field theoretic approach, the full set of stationary solutions contained in this article lays down the ingredients for a subsequent analysis of Schwinger effect in this framework (either through the S-matrix formalism [5,6] or with heat-kernel techniques [7]).

In spite of the similarity between $U(1)_\star$ and commutative Yang–Mills theories, constant chromoelectric fields do create gluons [8] whereas homogeneous fields do not produce photons in NC space (some aspects of photon propagation on homogeneous electromagnetic fields have been analyzed in [9] and [10]). For this reason, we study the propagation of photons across the interface of two regions, one with and the other without a background electric field. For simplicity, we take an electrostatic potential that only varies along a fixed spatial direction, and such that an homogeneous electric field is suddenly built up: NC space gets then split into halves by a flat interface. Next, we study the propagation of fluctuations of this background.

More specifically, our setting is the following. We start with $(d+1)$-dimensional Moyal spacetime, whose coordinates satisfy $[\hat{x}^\mu, \hat{x}^\nu] = 2i\theta^{\mu\nu}$, where $\theta^{\mu\nu}$ are elements

[a] e-mail: dascanio@fisica.unlp.edu.ar
[b] e-mail: pisani@fisica.unlp.edu.ar (corresponding author)
[c] e-mail: ulises2357@hotmail.com

of a real antisymmetric matrix. For simplicity, we take the time coordinate x^0 as an ordinary commuting parameter, i.e., $\theta^{\mu 0} = 0$. We then introduce a particular background, namely, a static electric field which vanishes on the left half-space $\hat{x}^1 < 0$, takes a constant value on the right half-space $\hat{x}^1 > 0$, and is perpendicular to the interface $\hat{x}^1 = 0$. The potential $A_0 = -E(|\hat{x}^1| + \hat{x}^1)/2$ generates such a step-like field; the constant E gives the electric field.

Due to the self-interaction introduced by noncommutativity, photons are scattered by this background. However, as will be shown, in the Moyal representation the interface effectively acts as a step of finite width with (depending on the polarization) delta-functions at the boundaries. This step scatters oblique incident photons; perpendicular beams do not experience any interaction with the electric field. According to the intensity of the background field, the energy and the direction of the incident photons one recognizes different regimes. Apart from the usual scattering – where incident photons split into partially transmitted and reflected light beams – one also finds, for a background which is not particularly strong, the propagation of edge states (viz. localized along the interface). Bound states as perturbations of solitonic solutions have already been found in [11].

On the other hand, for extremely intense electric fields (roughly, $|E| \sim 1/|\theta^{\mu\nu}|$) a realization of the Klein paradox arises. Our result for the scattering of vector particles is similar to the usual (i.e., commutative) Klein paradox for scalar particles [12]: the reflection coefficient R for a wave packet is greater than one. This would indicate that at the boundary of regions with strong electric fields photon beams could be produced.

There is an interesting result of our calculations that concerns two different manifestations of the Klein paradox. As is well-known, a reflection coefficient R greater than one is found either for monochromatic solutions of Dirac equation or for localized solutions of Klein–Gordon equation. In both cases this is considered as a sign of particle creation. At the same time, one finds (both for spinor and scalar particles) the paradoxical result that the transmission coefficient T does not vanish for infinitely strong barriers [13]. In the problem studied in this article we find $R > 1$ (for a localized packet) but, on the other hand, $T \to 0$ as the background field grows to infinity. This shows that these two aspects are not necessarily connected. It also suggests the need to perform a second quantized approach to reliably determine the rate of photon production.

Another aspect which is usually considered in the Klein regime is the divergence of the transmission coefficient for some value of the incident energy; this is usually called super-Klein tunneling (see e.g. [14]). For a bosonic field colliding against an abrupt step this occurs at incident energy equal to half the step height. In our setting there is no super-Klein tunneling, i.e., the transmission coefficient remains finite. The reason lies in the smearing introduced by noncommutativity which turns the abrupt edge into a region of finite slope (cf. [12]).

All these features of photon propagation are analyzed in the present article both for TE as well as for TM modes; sometimes called s-polarized and p-polarized waves, respectively. The former are not affected by gauge transformations; for the latter we choose the temporal gauge. Interestingly, this gauge choice introduces a singular background in the equation of motion. We show that this is a general picture in the Klein regime – independently of the background profile. However, the origin of the singularity can be clearly identified and its consequences removed.

Since its discovery [15], the Klein paradox has been thoroughly analyzed from different perspectives. Many aspects of its relation with particle creation in quantum field theory have been thoroughly discussed – we mention, e.g., [16–21]. More recently, techniques based on the space-time resolved solutions have provided further insight into the behavior of such systems (see, e.g., [22–25]). We think that the example considered in this article gives interesting information on the Klein paradox in a different setup, namely, one with propagating photons under nonlocal interactions. Moreover, for a specific photon polarization, we are lead to the problem of a single scalar field colliding against a step of finite width.[1] We consequently analyze some aspects of the solutions which, to the best of our knowledge, have not been studied before (see [27]).

Although our explicit solutions and their properties were obtained for a specific electric background, many calculations were carried out for a generic potential $A_0(x^1)$ so some qualitative aspects of the propagation of perturbations can be also inferred for more general background profiles – as long as they vary along a unique direction. In particular, some results still hold for a smoothed version of our setting, in which the interface where the electric background changes abruptly from zero to a finite value is replaced by a region of finite width. Further details in this respect are given in Sect. 10.

In the last section before our conclusions we also address, for comparison, the case of an interface which limits a region supporting an homogeneous static magnetic background. As in the case of the electric background, the scattering of photons due to the magnetic field ends up restricted within a small region around the interface. The explicit solutions for the magnetic case can be read from the analysis of the electric background but, as expected, their physical implications are quite different. In particular, no Klein paradox is observed.

Our article is organized as follows. In Sect. 2 we briefly review the construction of $U(1)_\star$ and focus on the dynamics of fluctuations around a classical background. In Sect. 3 we

[1] This is the scalar version of Sauter's seminal paper [26].

introduce our specific background and perform the decoupling between TE and TM modes. In Sect. 4 we identify the different regimes according to the energy of the incident beam. Sections 5 and 6 are devoted to the study of TE and TM modes, respectively. Singularities arising in the Klein region are resolved in Sect. 7. In Sect. 8 we analyze the existence of edge states. In Sect. 9 the case of a magnetic background is briefly discussed. Finally, in Sect. 10, we draw our conclusions.

2 Electrodynamics in Moyal spacetime

A natural procedure to set up a $(d+1)$-dimensional NC spacetime[2] is to introduce Hermitian operators $\hat{x}^\mu$ (with $\mu = 0, \ldots, d$) such that

$$[\hat{x}^\mu, \hat{x}^\nu] = 2i\theta^{\mu\nu}. \tag{2.1}$$

The real constants $\theta^{\mu\nu}$ represent minimal measurable areas, according to the uncertainty relation $\Delta x^\mu \Delta x^\nu \geqslant |\theta^{\mu\nu}|$. In other words, commutation relation (2.1) implies that states whose x^μ coordinate is localized within a small scale, say L, get smeared along a distance $\sim |\theta^{\mu\nu}|/L$ in the x^ν-direction. This phenomenon leads to the famous UV/IR mixing which jeopardizes renormalizability due to the low-momentum divergence of the one-loop propagator of virtual particles [28] (see also [29,30]).

As functions of the coordinate operators $\hat{x}^\mu$, classical fields $\phi(\hat{x})$ furnish a NC algebra which can be put in one-to-one correspondence with the space of ordinary functions $\phi(x)$ on $\mathbb{R}^{d+1}$, henceforth called Moyal spacetime. This map can be established through the Weyl–Wigner transform,

$$\phi(\hat{x}) = \int \frac{d^{d+1}x\, d^{d+1}p}{(2\pi)^{d+1}}\, e^{ip(\hat{x}-x)}\, \phi(x), \tag{2.2}$$

which produces the totally symmetric ordering in the operators $\hat{x}^\mu$. We use $\hat{x}^\mu$ to denote NC coordinates and unhatted x^μ for the ordinary commuting coordinates of Moyal spacetime. Under this correspondence the composition of operators is mapped into the Groenewold–Moyal product of functions, defined as

$$\begin{aligned}\phi(\hat{x})\cdot\psi(\hat{x}) \leftrightarrow \phi(x)\star\psi(x) &= \phi(x^\mu + i\theta^{\mu\nu}\partial_\nu)\,\psi(x)\\ &= \psi(x^\mu - i\theta^{\mu\nu}\partial_\nu)\,\phi(x).\end{aligned} \tag{2.3}$$

This representation can be readily checked, for example, on the original commutator $[x^\mu, x^\nu] = x^\mu \star x^\nu - x^\nu \star x^\mu = 2i\theta^{\mu\nu}$. Although not commutative, this product inherits the associativity of the composition of operators.

To construct an action in terms of the trace of an Hermitian operator we first note that any cyclic trace in the algebra of operators $\phi(\hat{x})$ gives, up to a normalization factor, the integral on $\mathbb{R}^{d+1}$ of the corresponding function of the fields $\phi(x)$ on Moyal spacetime [2]. In short, the NC generalization of a field theory is obtained by replacing in the action every ordinary multiplication by the Moyal $\star$-product.

Since the composition of two operators commute under a trace, noncommutativity does not alter the tree-level propagators but only plays a role in interaction terms. Most importantly, the NC generalization of local field theories turns out to be nonlocal because interactions become, roughly speaking, smeared over distances of order $\sqrt{|\theta^{\mu\nu}|}$. As we will see next, invariance under nonlocal gauge transformations turns NC electrodynamics into a self-interacting theory.

As in the commutative case, the symmetry $U(1)_\star$ is implemented through the covariant derivative

$$D_\mu = \partial_\mu + iA_\mu \tag{2.4}$$

that introduces a gauge field $A_\mu(x)$. A gauge transformation of this field is defined as

$$A_\mu \to U(x)\star A_\mu \star U^\dagger(x) - iU(x)\star\partial_\mu U^\dagger(x), \tag{2.5}$$

where $U(x)$ can be written as

$$U(x) = e_\star^{i\alpha(x)} = 1 + i\alpha(x) - \frac{1}{2}\,\alpha\star\alpha + \cdots \tag{2.6}$$

and $U(x)\star U^\dagger(x) = 1$. Under this transformation, $D_\mu \to U\star D_\mu \star U^\dagger$. In the sequel only gauge fields will be considered so in all cases the covariant derivative will act in the adjoint representation. Consequently, for notational convenience, from now on the action of D_μ should be understood as $[D_\mu, \cdot\,]$, where, of course, the commutator is computed with the $\star$-product.

The commutator $[D_\mu, D_\nu] = i[F_{\mu\nu}, \cdot\,]$ defines the covariant field strength

$$F_{\mu\nu} = \partial_\mu A_\nu - \partial_\nu A_\mu + i\,[A_\mu, A_\nu], \tag{2.7}$$

which clearly shows the resemblance between electromagnetism in Moyal spacetime and ordinary Yang–Mills theories. Under the gauge transformation (2.5) the field strength changes as $F_{\mu\nu} \to U\star F_{\mu\nu}\star U^\dagger$.

As briefly explained above, the generalization of Maxwell action to Moyal spacetime is simply given by

$$S[A] = \int d^{d+1}x\, \left(-\frac{1}{4}\,F^{\mu\nu}\star F_{\mu\nu} - J^\mu \star A_\mu\right). \tag{2.8}$$

[2] We adopt the mostly minus signature $\eta = (+ - \cdots -)$.

Upon integration by parts the $\star$-product can be removed from quadratic terms in the action but it must be retained in cubic and quartic self-interactions. To introduce in our setting a background electric field we have included a fixed external source $J^\mu(x)$. Due to the cyclicity of the Moyal product under the integral sign, in the absence of an external source the action (2.8) is $U(1)_\star$ invariant.

At the classical level, several works on the dynamics of matter on external gauge field configurations can be found in the literature: the hydrogen atom [31], Stark and Zeeman effects [31], Landau problem [32–36], Aharonov–Bohm effect [37–42], quantum Hall effect [39,41,43], Aharonov–Casher effect [44], the Dirac quantization condition [45]. In this article we consider instead a static charge configuration which acts as the source J^μ in (2.8) of a fixed A_μ and study the dynamics of perturbations around this specific solution for the gauge field.

The equation of motion

$$D_\mu F^{\mu\nu} = J^\nu \tag{2.9}$$

determines the configuration of the gauge field for any given external source. An immediate implication of (2.9) is that the current must be covariantly constant,

$$D_\mu J^\mu = 0. \tag{2.10}$$

Let us now assume a specific solution $A_\mu(x)$ and introduce small fluctuations $a_\mu(x)$ around this background. If we write the full gauge field as $A_\mu(x) + a_\mu(x)$, the (linearized) field tensor becomes

$$F_{\mu\nu} + D_\mu a_\nu - D_\nu a_\mu. \tag{2.11}$$

In this expression and hereafter, $F_{\mu\nu}$ and D_μ are computed exclusively in terms of the background field A_μ. Replacing (2.11) into (2.9) we obtain the linearized equation of motion for the perturbations,

$$-\eta_{\mu\nu}\, D^2 a^\nu + D_\mu D_\nu a^\nu - 2i\,[F_{\mu\nu}, a^\nu] = 0. \tag{2.12}$$

Note also that, since J^μ is the same for A_μ and $A_\mu + a_\mu$, condition (2.10) now implies

$$[a_\mu, J^\mu] = 0. \tag{2.13}$$

Before considering in detail a specific background, let us examine gauge invariance on the perturbations. In the presence of a background field, gauge invariance remains as a small $U(1)_\star$ symmetry on the fluctuations,

$$\delta a_\mu = D_\mu \alpha(x), \tag{2.14}$$

that preserves their equation of motion as long as

$$0 = [D_\mu F^{\mu\nu}, \alpha] = [J^\nu, \alpha]. \tag{2.15}$$

Therefore, we can conveniently gauge the perturbations with a parameter $\alpha(x)$ that commutes with the external source.

3 The background

Let us define our specific setup. As already mentioned, we are interested on the effects of spatial noncommutativity, so we take the time coordinate x^0 as a commuting variable [46,47]. As for the space coordinates, note that after an appropriate choice the antisymmetric matrix $\theta^{\mu\nu}$ can be diagonalized in 2×2 blocks. In this way, space becomes decomposed into several Moyal planes such that coordinates from different planes commute with each other. For our purposes it is enough to distinguish the coordinates x^1, x^2 of one of these planes from the remaining $d-2$ spatial coordinates. Noncommutativity is then characterized by a positive parameter θ through

$$[x^1, x^2] = 2i\theta \tag{3.1}$$

together with a $(d-2) \times (d-2)$ antisymmetric matrix in the rest of Moyal space. As will become evident soon, if the background does not depend on these $d-2$ coordinates then this antisymmetric matrix is irrelevant.

We now introduce a background $A_0 = A_0(x^1)$ that varies only along the direction of x^1, and set the spatial components to zero: $A_1 = \cdots = A_d = 0$. We will shortly choose a specific x^1-dependence for A_0. This static background represents a purely electric field $E(x^1) = -A_0'(x^1)$ in the x^1–direction, and originates on a static distribution of charge density $J^0 = -A_0''(x^1)$; spatial components of the current vanish as well, $J^1 = \cdots = J^d = 0$.

Since the static background does not change with the transverse coordinates $x_\perp = (x^2, \ldots, x^d)$, we analyze fluctuations that propagate with fixed energy k^0 and transverse momentum $k_\perp = (k^2, \ldots, k^d)$,

$$a_\mu(x) = a_\mu(x^1)\, e^{-ik^0x^0 + ik_\perp x_\perp}. \tag{3.2}$$

Here, $k_\perp x_\perp = k^2x^2 + \cdots + k^dx^d$.

It is now important to point out that the commutator between any background which only depends on x^1 and any field with definite momentum k^2 can be written as an ordinary multiplication between the same field and another function which, roughly, evaluates the variation of the original function at distances $\Delta x^1 \sim \theta k^2$. For example,

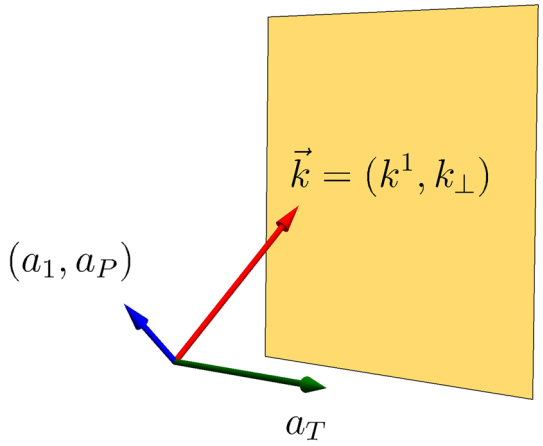

Fig. 1 Decomposition of the gauge field into TE modes a_T (green) and TM modes a_1, a_P (blue)

$$[A_0(x^1), a_\mu(x^1)\, e^{-ik^0x^0+ik_\perp x_\perp}] = \delta A_0(x^1)\, a_\mu(x^1) \times e^{-ik^0x^0+ik_\perp x_\perp}, \tag{3.3}$$

with

$$\delta A_0(x^1) = A_0(x^1 - \theta k^2) - A_0(x^1 + \theta k^2). \tag{3.4}$$

This expression shows that if $k_\perp$ has no component in the direction of x^2 the background is transparent to photon beams. As already mentioned, since the background only depends on x^1, the propagation of photons will only be affected by θ, and the remaining NC parameters will have no physical consequence.

Before solving (2.12) for our specific background, let us establish some convenient notation. We decompose the fluctuations $a_\mu = (a_0, \ldots, a_d) = (a_0, a_1; a_\perp)$ as follows. In an asymptotic region – where the background eventually vanishes – the fluctuations propagate with momentum $\vec{k} = (k^1, \ldots, k^d) = (k^1; k_\perp)$; as expected, in the absence of a background the wave equation (2.12) indicates that the spatial part of a_μ is perpendicular to $\vec{k}$. We separate from the transverse field $a_\perp$ two components: (i) the projection a_P in the plane of incidence (i.e., the component parallel to $k_\perp$), and (ii) a_T, which is a $(d-3)$-component vector perpendicular to the direction of x^1 and to $k_\perp$. This decomposition is illustrated in Fig. 1 for an incoming wave entering a region of non-vanishing background (represented by the flat surface).

With some abuse of notation,

$$a_\mu = a_0 \oplus a_1 \oplus a_P \oplus a_T. \tag{3.5}$$

In the asymptotic region the electric field of an incoming wave is proportional to the spatial components of the gauge field. Therefore, a_1, a_P describe a beam with electric field in the plane of incidence (TM mode or p-polarized wave). On the other hand, the components a_T give an electric field perpendicular to the plane of incidence (TE mode or s-polarized wave).

Through the equation of motion (2.12) each component of a_T gets completely decoupled,

$$\left[(k_0 - \delta A_0)^2 - |k_\perp|^2 + \partial_1^2\right] a_T = 0. \tag{3.6}$$

TM modes then satisfy Klein–Gordon equation for a charged field of mass $|k_\perp|$ in interaction with an electrostatic potential $\delta A_0(x^1)$. After choosing a specific background δA_0 we will solve this equation in Sect. 5.

The remaining components $a_0(x^1), a_1(x^1), a_P(x^1)$ satisfy the coupled equations

$$a_0'' - |k_\perp|^2 a_0 - (k_0 - \delta A_0)\left(i a_1' - |k_\perp|\, a_P\right) + 2i\delta A_0'\, a_1 = 0, \tag{3.7}$$

$$\left[(k_0 - \delta A_0)^2 - |k_\perp|^2\right] a_1 + i(k_0 - \delta A_0) a_0' - i|k_\perp| a_P' + i\delta A_0'\, a_0 = 0, \tag{3.8}$$

$$(k_0 - \delta A_0)^2 a_P + a_P'' - |k_\perp|\left[(k_0 - \delta A_0) a_0 + i a_1'\right] = 0. \tag{3.9}$$

These equations imply condition (2.13), which can now be written as $\delta J^0\, a_0 = 0$ or, equivalently, as $\delta A_0''\, a_0 = 0$. Under this condition any two equations among (3.7)–(3.9) imply the third one. Consequently, we will choose the temporal gauge $a_0 = 0$, which trivially satisfies (2.13), and will use (3.7) and (3.8) to find a_1 and a_P. This will be done in Sect. 6.

Now it is time to choose a specific profile for the background $A_0(x^1)$: We take a slope that begins abruptly at $x^1 = 0$ (as in Fig. 2),

$$A_0(x^1) = \begin{cases} 0 & x^1 < 0 \\ -E\, x^1 & x^1 > 0 \end{cases}. \tag{3.10}$$

The parameter $E \in \mathbb{R}$ gives the intensity of the electric field. From the viewpoint of the NC spacetime, this potential represents the boundary of a region supporting a static homogeneous electric field. This setting can be considered as a first approach to the study of the dynamics of fluctuations at the interface where an electric field is built up.

Recall that, according to (3.3), the action of $A_0(x^1)$ on oscillations (3.2) turns the slope-like potential into a broadened step of small width $2L$ (Fig. 3), with

$$L = \theta|k^2|. \tag{3.11}$$

In fact, inserting (3.10) into (3.4) one obtains

$$\delta A_0(x^1) = \begin{cases} 0 & x^1 < -L \\ -E(x^1 + L) & |x^1| < L \\ -2EL & x^1 > L \end{cases}. \tag{3.12}$$

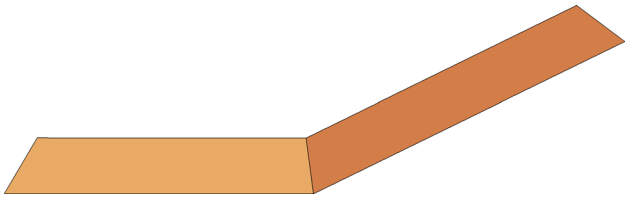

Fig. 2 Background slope from the NC spacetime perspective. In the picture $E < 0$ so the electric field points towards the left

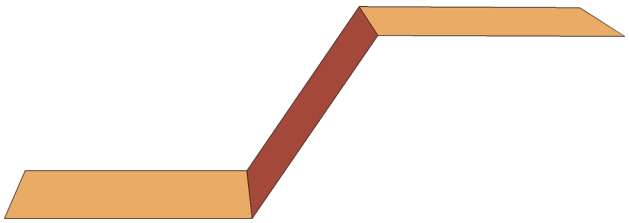

Fig. 3 The background as it interacts with incoming photons (for $\text{sign}(k^2)E > 0$). The width of the step depends on the transverse momentum k^2; its slope, on the electric field E

In this expression and in the rest of this article we assume $\text{sign}(k^2) < 0$; if the component k^2 is positive one simply changes the sign of E. Correspondingly, the adjoint action of the electric field is given by

$$[F_{01}, \cdot\,] = -\delta A_0'(x^1) = \begin{cases} 0 & |x^1| > L \\ E & |x^1| < L \end{cases} . \tag{3.13}$$

This shows that photons effectively interact with the electric field only in a narrow region of width $2L$.

Correspondingly, the homogeneous background on the half-plane is generated by a charge density $J^0 = \frac{1}{2} E\, \delta(x^1)$ together with a second parallel plate of opposite charge density and located at $x^1 = +\infty$. Condition $\delta J^0\, a_0 = 0$ now forces a_0 to vanish at the edges of the step.

4 Energy regimes

Fluctuations (3.2) are characterized by their energy k_0 and their transverse momentum $k_\perp$. As already mentioned, photons incident normally to the interface – or even with no k^2 component – do not interact with the background. Let us call β the angle between the plane of incidence and the x^1x^2-plane. One can distinguish, both for TE and TM modes, different energy regimes according to the intensity of the electric field: (i) very strong electric fields such that $\theta|E|\cos\beta > 1$, and (ii) ordinary electric fields for which $\theta|E|\cos\beta < 1$.

Case (i) is represented in Figs. 4 and 5 for $E < 0$ and $E > 0$, respectively. The transverse momentum $k_\perp$ introduces a mass gap. Accordingly, five different energy regimes can be identified: the blue lines represent photons with positive or negative energy that collide against the step-like background and generate reflected and transmitted waves; this we call the *propagation region*. Orange dashed lines represent photons which propagate only at one side of the interface with an energy that lies within the mass gap at the other side. Therefore, the photon does propagate across the interface and suffers a total reflection. Finally, there exists a finite interval of energies, usually called *Klein zone*, for which the incident photon lies above and below the surface of the Dirac sea, depending on the side of the step. This is represented by the red horizontal lines in the figures. In this regime particles (with positive kinetic energy) at one side of the step are seen as antiparticles (with negative kinetic energy) at the other side.

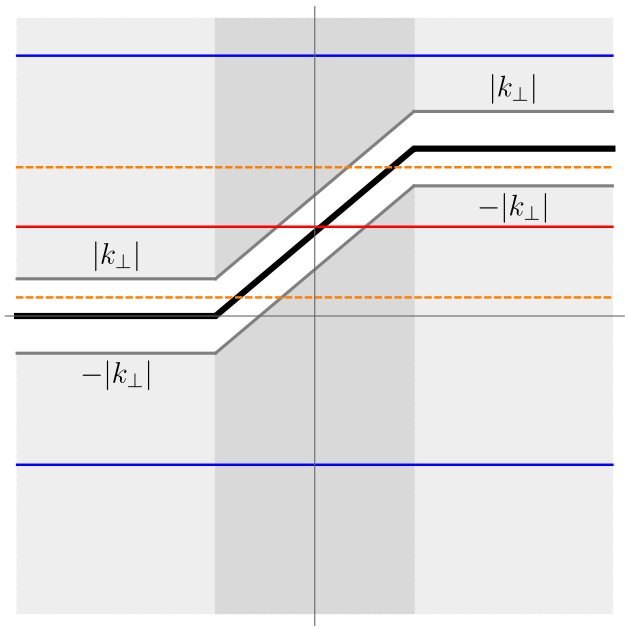

Fig. 4 The black solid line represents the potential δA_0 for a strong electric field $E < 0$. Horizontal lines correspond to five different energy regimes

In case (ii) one also finds the usual propagation region but the electric field is not strong enough to separate the mass gaps and generate a Klein zone. As a consequence, there is an overlapping between the mass gaps at either side of the interface so that one could eventually find states localized close to this surface (edge states). This possibility will be analyzed in Sect. 8.

5 TE modes

We begin by solving equation of motion for TE modes a_T. Recall that each of the $d-2$ components – which we now generically denote as $\phi(x^1)$ – satisfies the Klein–Gordon equation for a charged scalar field of mass $|k_\perp|$ scattered by an electrostatic potential δA_0. Taking into account the piecewise

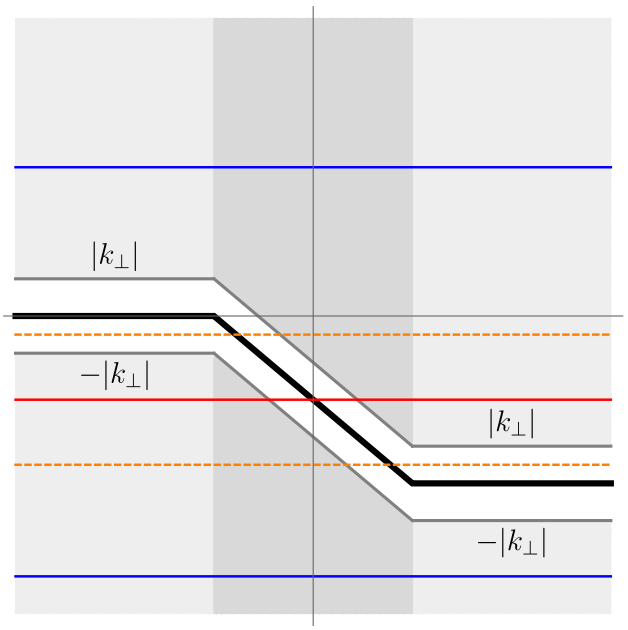

Fig. 5 The black solid line represents the potential δA_0 for a strong electric field $E > 0$. Horizontal lines correspond to five different energy regimes

definition of $\delta A_0(x^1)$, we solve (3.6) by appropriately matching at $x^1 = \pm L$ the solutions in the left region $x^1 < -L$, the right region $x^1 > L$, and the intermediate region $|x^1| < L$. These we denote by ϕ_L, ϕ_R and ϕ_I, respectively.

In the regions $|x^1| > L$ the background δA_0 is constant so the solutions are simply incoming and outgoing plane waves at either side of the step,

$$\phi_L(x^1) = a\, e^{ik^1 x^1} + b\, e^{-ik^1 x^1} \qquad \text{for } x^1 < -L, \tag{5.1}$$

$$\phi_R(x^1) = c\, e^{i\kappa^1 x^1} + d\, e^{-i\kappa^1 x^1} \qquad \text{for } x^1 > L, \tag{5.2}$$

with

$$k^1 = +\sqrt{k_0^2 - |k_\perp|^2}, \tag{5.3}$$

$$\kappa^1 = +\sqrt{(k_0 + 2EL)^2 - |k_\perp|^2}. \tag{5.4}$$

In the intermediate region $|x^1| < L$ the function δA_0 is linear in x^1 so the field satisfies

$$-\phi_I'' + \left(|k_\perp|^2 - E^2 z^2\right)\phi_I = 0, \tag{5.5}$$

where we have shifted the x^1 coordinate as

$$z = x^1 + L + \frac{k_0}{E}. \tag{5.6}$$

The solutions can be written as

$$\phi_I(x^1) = A\, F(x^1) + B\, G(x^1) \qquad \text{for } -L < x^1 < L, \tag{5.7}$$

in terms of parabolic functions

$$F(x^1) = \frac{\Gamma(-\nu)}{\sqrt{2i|E|}}\Big[D_\nu(-\sqrt{2i|E|}\,\tfrac{k0}{E})D_\nu(\sqrt{2i|E|}z) - D_\nu(\sqrt{2i|E|}\,\tfrac{k0}{E})D_\nu(-\sqrt{2i|E|}z)\Big], \tag{5.8}$$

$$G(x^1) = \Gamma(-\nu)\Big[D_\nu'(-\sqrt{2i|E|}\,\tfrac{k0}{E})D_\nu(\sqrt{2i|E|}z) + D_\nu'(\sqrt{2i|E|}\,\tfrac{k0}{E})D_\nu(-\sqrt{2i|E|}z)\Big], \tag{5.9}$$

where $\nu = -1/2 + ik_\perp^2/2|E|$. These particular combinations were chosen to satisfy $F(-L) = G'(-L) = 0$ and $F'(-L) = G(-L)$.

After imposing continuity of ϕ and its derivative at $x^1 = \pm L$ one obtains four equations: two of them give the coefficients A, B in the intermediate region in terms of a, b, c, d; the remaining two equations determine the elements of the S-matrix,

$$S = \begin{pmatrix} t_L & r_R \\ r_L & t_R \end{pmatrix}, \tag{5.10}$$

that relates the outgoing coefficients b, c with the incoming coefficients a, d through

$$\begin{pmatrix} \sqrt{\kappa^1}\, c \\ \sqrt{k^1}\, b \end{pmatrix} = S \begin{pmatrix} \sqrt{k^1}\, a \\ \sqrt{\kappa^1}\, d \end{pmatrix}. \tag{5.11}$$

A straightforward calculation gives

$$r_{L,R} = \frac{i\kappa^1\left(ik^1 F_L \pm G_L\right) \mp ik^1 F_L' - G_L'}{i\kappa^1\left(ik^1 F_L - G_L\right) - ik^1 F_L' + G_L'}\, e^{-2ik_{L,R}L}, \tag{5.12}$$

$$t_{L,R} = \frac{\sqrt{8\pi k^1 \kappa^1}\, i}{i\kappa^1\left(ik^1 F_L - G_L\right) - ik^1 F_L' + G_L'}\, e^{-i(k_L + k_R)L}. \tag{5.13}$$

The upper (lower) sign corresponds to r_L (r_R). We have also defined $k_L = k^1$ and $k_R = \kappa^1$. We use F_L, G_L to denote $F(L)$, $G(L)$, and similarly for the derivatives.

Relation (5.11) parametrizes the two-dimensional space of solutions. The coefficients a and d represent incoming waves from the left and from the right, respectively. Thus, if $d = 0$ then b is related to the reflection coefficient and c to the transmission coefficient of a wave colliding the step from the left. Correspondingly, $a = 0$ describes a wave colliding from the right and the roles of b and c get interchanged. To

define reflection and transmission coefficients we compute the conserved current[3]

$$J(x^1) = \mathrm{Im}\,(\phi^*\phi'), \tag{5.14}$$

which according to (3.6) must be x^1-independent. For $x^1 < -L$, expression (5.1) gives

$$J = \mathrm{Re}(k^1)\Big[|a|^2 e^{-2x^1 \mathrm{Im}(k^1)} - |b|^2 e^{2x^1 \mathrm{Im}(k^1)}\Big] - 2\,\mathrm{Im}(k^1)\,\mathrm{Im}\Big[ab^* e^{2ix^1 \mathrm{Re}(k^1)}\Big]. \tag{5.15}$$

The same expression holds for $x^1 > L$ if one makes the following replacements: $k^1 \to \kappa^1$, $a \to c$ and $b \to d$.

For energies in the propagation and in the Klein regimes both k^1 and κ^1 are positive real numbers, so current conservation $J(-\infty) = J(+\infty)$ implies

$$k^1|a|^2 - k^1|b|^2 = \kappa^1|c|^2 - \kappa^1|d|^2. \tag{5.16}$$

This expression – valid for arbitrary values of the constants a, d – proves that S is a unitary matrix. Further relations between the elements of the S-matrix can be obtained by noting that the complex conjugates of (5.1) and (5.2) provide another stationary solution but where the roles of b, c and a, d are played by a^*, d^* and b^*, c^*, respectively. This implies $t_R = t_L$ and $|r_L| = |r_R|$. Although these relations can be readily checked in (5.12) and (5.13), their derivation did not make use of the specific form of the background. In fact, this is a well-known result from one-dimensional scattering: reflection (and transmission) coefficients for left- or right-incident waves coincide.

Reflection and transmission coefficients are then defined as $R = |r_L|^2 = |r_R|^2$ and $T = |t_L|^2 = |t_T|^2$. Unitarity of S implies $R + T = 1$. Figure 6 displays R as a function of the incident energy k_0.

The reflection coefficient decreases monotonically from 1 to 0 with increasing $|k_0|$. If the energy lies within one of the mass gaps then either k^1 or κ^1 are pure imaginary so $J = 0$ and the incoming photon is totally reflected at the interface ($R = 1$).

In the Klein zone R is smaller than 1 but to get an appropriate interpretation of the reflection coefficient it is crucial to recall that for these energies phase and group velocities have opposite signs. Let us consider, for example, the case $E < 0$ (Fig. 4). For incident energies $|k_\perp| < k_0 < -2EL - |k_\perp|$ both momenta k^1 and κ^1 are real but the group velocity at $x^1 > L$ is

$$v = \frac{dk_0}{d\kappa^1} = \frac{\kappa^1}{k_0 + 2EL} < 0. \tag{5.17}$$

[3] This current corresponds to the conserved (canonical) momentum of the electromagnetic field. This issue is discussed in Sect. 10.

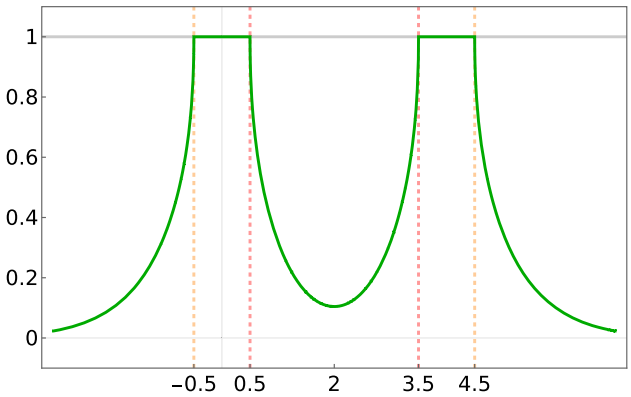

Fig. 6 R vs. k_0 for monochromatic TE modes ($|E|\theta\cos\beta > 1$ and $E < 0$). In this picture $k_2 = 0.25$, $k_\perp = 0.5$, $E = -8$ in length units of $\sqrt{\theta}$

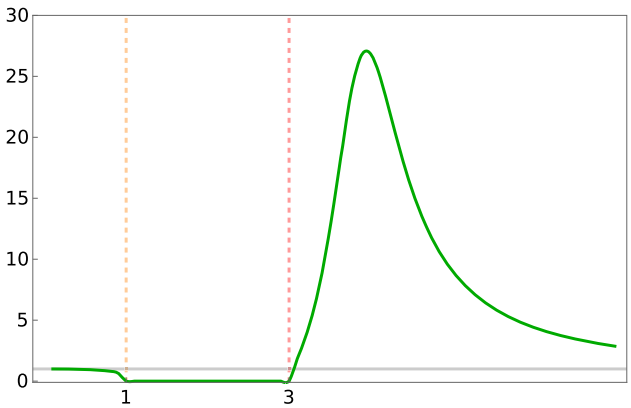

Fig. 7 T vs. $|E|$ for a pulse of TE modes. At the left of the orange dashed line lies the propagation zone; at the right of the red dashed line, the Klein zone. In this picture $E < 0$, $k_2 = 0.25$, $k_\perp = 0.5$, $k_0 = 1$ in length units of $\sqrt{\theta}$

Therefore, the stationary solutions which are relevant to model the scattering of a left-incident wave packet are not obtained by choosing $d = 0$ in (5.1) and (5.2) but instead by taking $c = 0$. The reflection and transmission coefficients are then given by $R = 1/|r_L|^2$ and $T = |t_L|^2/|r_L|^2$ and the relation $R = 1 + T > 1$ holds. This is the Klein paradox which is interpreted as the result of a total reflection of the incident packet together with the creation of pairs of photons at the interface at a rate T.

Alternatively, the term "Klein paradox" is sometimes used to refer to the existence of a non-vanishing transmission coefficient even for a infinitely high barrier – this is the case for a Klein–Gordon or Dirac particle colliding an ordinary abrupt step. Interestingly, this does not happen in our setting. In fact, the leading behavior of (5.8) and (5.9) for large $|E|$ reads [48]

$$F(x^1) \sim -\Gamma\left(\tfrac{1}{4}\right) z^{-\frac{1}{2}} |E|^{-\frac{3}{4}} \sin\left(\tfrac{1}{2}z^2|E| + \tfrac{\pi}{8}\right), \tag{5.18}$$

$$G(x^1) \sim -2\Gamma\left(\tfrac{3}{4}\right) z^{-\frac{1}{2}} |E|^{-\frac{1}{4}} \cos\left(\tfrac{1}{2}z^2|E| - \tfrac{\pi}{8}\right). \tag{5.19}$$

Consequently, the behavior of T for large values of the electric field is given by

$$T = \frac{|t_L|^2}{|r_L|^2} \sim \frac{2\pi k^1}{\left[\Gamma(\frac{3}{4})\right]^2 \sqrt{|E|}}. \tag{5.20}$$

The dependence of T on the electric field E is shown in Fig. 7 for a wave packet. In the propagation region $0 < T < 1$. If the energy of the packet falls in the mass gap then $T = 0$. For strong backgrounds, T may be even greater than 1 – the transmitted pulse is interpreted as photons created at the step. Nevertheless, $T \to 0$ as $|E| \to \infty$.

Finally, let us recall that for an ordinary scalar field pulse colliding against an abrupt step (i.e., a step of zero width) the coefficients R and T diverge if the energy is half the step height – this is usually known as super-Klein tunneling. However, the reflection coefficient shown in Fig. 6 (for a monochromatic wave) does never vanish so the corresponding coefficient for the wave packet (obtained by replacing $R \to 1/R$) does not diverge. This is a consequence of the smearing of the step in Moyal space. In the limit case $\theta \to 0$ and $|E| \to \infty$ (with $|E|\theta$ finite) one obtains and abrupt step and the reflection coefficient for a monochromatic wave certainly vanishes if its energy is exactly half the step height and one recovers super-Klein tunneling in this specific limit.

6 TM modes

Components a_T are unaffected by a gauge transformation (2.14) but to determine a_0, a_1, a_P we need to fix a specific gauge. We solve (3.7)–(3.9) by setting $a_0(x^1) = 0$ with an appropriate parameter of the form $\alpha(x) = \alpha(x^1)\, e^{-ik^0x^0+ik_\perp x_\perp}$. Condition (2.15) requires $\alpha(x^1)$ to vanish at the edges of the step $x^1 = \pm L$ but, since any solution $a_0(x^1)$ vanishes at those points, one can consistently choose α such that $a_0 + D_0\alpha = 0$.

For $a_0 = 0$ Eqs. (3.7) and (3.8) read

$$-(k_0 - \delta A_0)\left(ia_1' - |k_\perp|\, a_P\right) + 2i\,\delta A_0'\, a_1 = 0, \tag{6.1}$$

$$\left[(k_0 - \delta A_0)^2 - |k_\perp|^2\right] a_1 - i|k_\perp| a_P' = 0. \tag{6.2}$$

As already mentioned, (3.9) can be derived from these two equations. From (6.1) we eliminate the component which is parallel to the transverse momentum $k_\perp$,

$$-i|k_\perp| a_P = a_1' - 2\frac{\delta A_0'}{k_0 - \delta A_0}\, a_1. \tag{6.3}$$

The other component can be written as

$$a_1 = \frac{\varphi(x^1)}{k_0 - \delta A_0}, \tag{6.4}$$

where $\varphi(x^1)$ satisfies the Schrödinger-like equation

$$\phi'' - \left[k_\perp^2 - (k_0 - \delta A_0)^2 + \frac{2\delta A_0'^2}{(k_0 - \delta A_0)^2} + \frac{\delta A_0''^2}{k_0 - \delta A_0}\right]\phi = 0\,. \tag{6.5}$$

Up to now we have not used the explicit dependence of the background on x^1. For the step-like potential (3.12) the fourth term inside the square brackets only introduces delta-functions at the edges of the step,

$$\delta A_0'' = E\left[\delta(x^1 - L) - \delta(x^1 + L)\right]. \tag{6.6}$$

We now solve (6.5) in the same fashion as for the TE modes: we find a piecewise solution and match the coefficients by imposing the appropriate behavior at the edges of the step. At $x^1 < -L$ and $x^1 > L$ the field φ (respectively denoted by φ_L and φ_R) takes the form

$$\varphi_L = a\, e^{ik^1x^1} + b\, e^{-ik^1x^1}, \tag{6.7}$$

$$\varphi_R = c\, e^{i\kappa^1x^1} + d\, e^{-i\kappa^1x^1}, \tag{6.8}$$

with k^1 and κ^1 once more given by (5.3) and (5.4). At the interval $|x^1| < L$ the field (denoted by φ_I) satisfies

$$-\varphi_I'' + \left(|k_\perp|^2 - E^2z^2 + \frac{2}{z^2}\right)\varphi_I = 0, \tag{6.9}$$

where the variable z is the same as (5.6). It is interesting to make a comparison with the equation for the TM modes (5.5): the dynamics of TE modes contains an additional, singular term $1/z^2$. The effect of this term will be discussed in some detail.

Solutions to (6.9) can be written as combinations of the following confluent hypergeometric functions,

$$f_1(x^1) = \frac{1}{z}\, e^{-\frac{i}{2}|E|z^2}\, {}_1F_1\left(-\tfrac{1}{4} - \tfrac{i|k_\perp|^2}{4|E|}, -\tfrac{1}{2}; i|E|z^2\right), \tag{6.10}$$

$$f_2(x^1) = z^2\, e^{-\frac{i}{2}|E|z^2}\, {}_1F_1\left(\tfrac{5}{4} - \tfrac{i|k_\perp|^2}{4|E|}, \tfrac{5}{2}; i|E|z^2\right). \tag{6.11}$$

The field at the intermediate region is thus determined by two coefficients A, B,

$$\varphi_I = A\,\bar{F}(x^1) + B\,\bar{G}(x^1), \tag{6.12}$$

where now

$$\bar{F}(x^1) = -\tfrac{1}{3}\left[f_2(-L)\, f_1(x^1) - f_1(-L)\, f_2(x^1)\right], \tag{6.13}$$

$$\bar{G}(x^1) = \tfrac{1}{3}\left[f_2'(-L)\, f_1(x^1) - f_1'(-L) f_2(x^1)\right]. \tag{6.14}$$

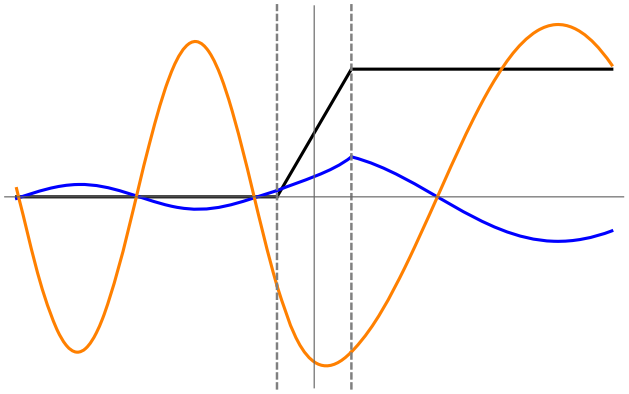

Fig. 8 Gauge field components a_1 (blue) and a_P (orange) with energy in the propagation regime. In black, the background field ($E < 0$). The delta-functions at $x^1 = \pm L$ introduce discontinuities in the derivatives

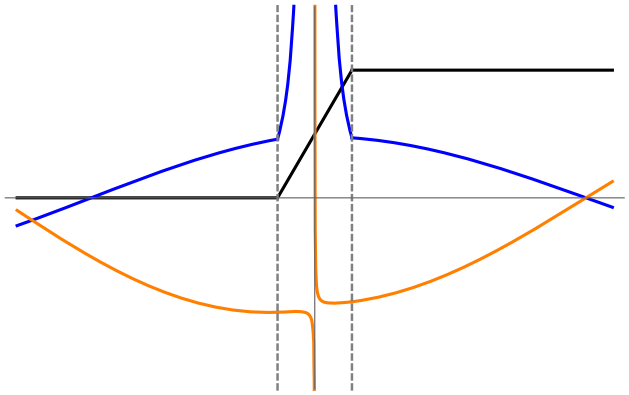

Fig. 9 Gauge field components a_1 (blue) and a_P (orange) with energy in the Klein regime. The background field (black) corresponds to $E < 0$. Due to the singularity in (6.9), the solutions diverge at $z = 0$

These particular solutions have been chosen such that $\bar{F}(-L) = \bar{G}'(-L) = 0$ and $\bar{F}'(-L) = \bar{G}(-L) = 1$.

Next, we match the behavior of $\varphi_L, \varphi_R, \varphi_I$ at the edges of the step to construct the full solution φ. We demand continuity of the wave function but, in accordance with (6.6), we introduce discontinuities on the derivatives. The matching conditions then read

$$\varphi_L(-L) = \varphi_I(-L), \tag{6.15}$$

$$\varphi_L'(-L) = \varphi_I'(-L) + \frac{E}{k_0}\,\varphi_I(-L), \tag{6.16}$$

$$\varphi_R(L) = \varphi_I(L), \tag{6.17}$$

$$\varphi_R'(L) = \varphi_I'(L) + \frac{E}{k_0 + 2EL}\,\varphi_I(L). \tag{6.18}$$

From these four equations we compute the elements $\bar{r}_L, \bar{r}_R$, $\bar{t}_L, \bar{t}_R$ of the S-matrix which, as in (5.11), relate outgoing with incoming coefficients,

$$\bar{r}_{L,R} = -\frac{\left(\frac{E}{k_0} \mp ik^1\right)\bar{F}_L' - \bar{G}_L' + \left(\frac{E}{k_0+2EL} \mp i\kappa^1\right)\left[\left(\frac{E}{k_0} \mp ik^1\right)\bar{F}_L - \bar{G}_L\right]}{\left(\frac{E}{k_0} + ik^1\right)\bar{F}_L' - \bar{G}_L' + \left(\frac{E}{k_0+2EL} - i\kappa^1\right)\left[\left(\frac{E}{k_0} + ik^1\right)\bar{F}_L - \bar{G}_L\right]}\, e^{-2ik_{L,R}L}, \tag{6.19}$$

$$\bar{t}_{L,R} = \frac{2i\sqrt{k^1\kappa^1}\, e^{-i(k_L+k_R)L}}{\left(\frac{E}{k_0} + ik^1\right)\bar{F}_L' - \bar{G}_L' + \left(\frac{E}{k_0+2EL} - i\kappa^1\right)\left[\left(\frac{E}{k_0} + ik^1\right)\bar{F}_L - \bar{G}_L\right]}. \tag{6.20}$$

As before, the upper (lower) sign corresponds to r_L (r_R); we define $k_L = k^1$ and $k_R = \kappa^1$ and we use $\bar{F}_L, \bar{G}_L, \bar{F}_L', \bar{G}_L'$ to denote $\bar{F}(L), \bar{G}(L), \bar{F}'(L), \bar{G}'(L)$.

Figure 8 shows the full solution for the gauge field components $a_1(x), a_P(x^1)$ with energy in the propagation regime. As expected, the wave is continuous but its derivative jumps at the edges of the step.

Figure 9 displays instead both components $a_1(x^1), a_P(x^1)$ in the case where the energy of the gauge field lies in the Klein zone. The most remarkable feature is the singularity at some $x^1 \in [-L, L]$. The obvious reason for this divergence is the singularity in the differential equation (6.9) at $z = 0$. For energies in the propagation region z never vanishes in the interval $x^1 \in [-L, L]$ but in the Klein regime there is some value of x^1 in this interval where $z = 0$. In consistence with Fig. 9, the component a_1 has a double pole, whereas a_P has a simple pole. We postpone to Sect. 7 a more detailed discussion of the physical origin of this divergence and a procedure to appropriately remove it.

Let us comment on the solutions (6.19) and (6.20). We have obtained $t_L = t_R$ and, since $\bar{F}, \bar{G}$ are real functions, one readily checks $|r_L| = |r_R|$, as long as $k^1, \kappa^1 \in \mathbb{R}$. The reflection coefficient for a monochromatic wave is then given by $R = |r_L|^2$. As before, unitarity of the S-matrix implies $R + T = 1$. Figure 10 shows the reflection coefficient as a function of the photon energy k_0.

The plot is similar to the one corresponding to TE modes but with a sudden decrease in the vicinity of the mass-gap regions, where $R = 1$. The figure shows that, in general, TE modes suffer a higher reflection than TM modes.

7 The Klein zone

Let us analyze the divergences that occur in the Klein zone for TM modes. The emergence of singularities stems from the covariant derivative $D_0 = \partial_0 + iA_0(x^1)$ which acting on

stationary solutions introduces the factor $k_0 - \delta A_0(x^1)$. In a typical Klein paradox scenario the potential attains asymptotically constant values $\delta A_0(\pm\infty)$; for intense backgrounds their difference $\delta A_0(+\infty) - \delta A_0(-\infty)$ exceeds the mass gap and thus the band of energies known as Klein zone is created. For k_0 within this band there is necessarily at least one point x^1 (assuming continuous backgrounds) such that $k_0 = \delta A_0(x^1)$, so the covariant derivative vanishes at this point. Decoupling the components of the gauge field in (3.7)–(3.9) then leads to the appearance of a singular term $(k_0 - \delta A_0)^{-2}$ in the equation of motion (third term in (6.5)).

To be more concrete, let us turn back to our background (3.12), which behaves as $\delta A_0 = -E(x^1 + L) = -Ez + k_0$ for $x^1 \in [-L, L]$. Therefore, $k_0 - \delta A_0 \sim z$. For any k_0 in the Klein zone the coordinate z vanishes at $x^1 = -L - k_0/E \in [-L, L]$. As a consequence, the field $\varphi(x^1)$ scatters against a singular background of the type z^{-2}. Close to a singularity of this type the solutions show two different behaviors: z^{-1} and z^2 (as shown by (6.10) and (6.11), respectively). The regular solution (6.11) leads to finite gauge field components $a_1(x^1), a_P(x^1)$ but How do we interpret the singular gauge field that arises from the solution (6.10)? The answer is that the singular behavior comes from a singular gauge transformation. Consider a (non-singular) solution of the set of equations (3.7)–(3.9) before any specific gauge choice. In general $a_0(x^1) \neq 0$ but we can impose the temporal gauge by choosing $\alpha(x^1)$ such that $D_0\alpha(x^1) = -i(k_0 - \delta A_0(x^1))\alpha(x^1) = -a_0(x^1)$. Therefore, in the Klein zone $\alpha(x^1)$ has a singularity at $x^1 = -L - k_0/E$. As a consequence, in this gauge the time component vanishes but the spatial components a_1, a_P become singular. In fact, since α has a simple pole at $z = 0$, the transformation $a_\mu \to a_\mu + D_\mu\alpha$ introduces a simple pole in a_P and double pole in a_1. This is precisely what one obtains if one inserts the solution $\varphi \sim z^{-1}$ into (6.3) and (6.4). Fortunately, it is not necessary to abandon this gauge choice: one can undo the singular gauge transformation from (6.12) to obtain a regular gauge field (Fig. 11) or, alternatively, one can keep the singular solution but choosing the appropriate behavior at $z = 0$. We choose the latter approach.

In general, one-dimensional scattering against a singularity detaches the solutions at both sides of the singular point unless a certain matching condition is specified. In other words, one could choose a certain value for the coefficients A, B at one side of the singularity and a different value at the other side. If one is interested – to give an example – in solutions of definite parity, then one should choose them such that only one of the solutions (6.10) or (6.11) remains. One could even choose $A = B = 0$ at one side of the singularity if it fits the physical setting. In our case, we must keep in mind that after removing the simple pole from the solution φ one must get regular fields a_0, a_1, a_P. Therefore, the values of both coefficients A, B must not change after crossing $z = 0$. This solves the ambiguity that arises due to the singularity

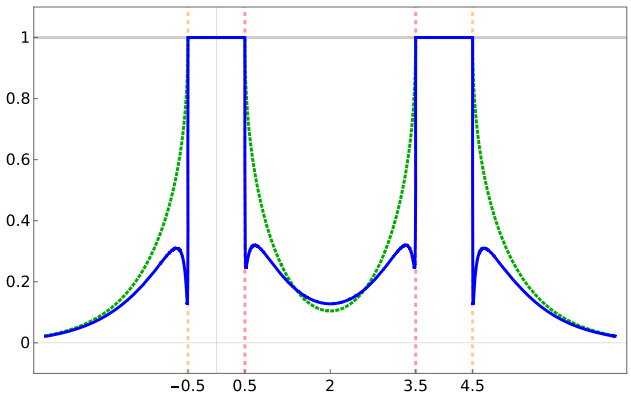

Fig. 10 R vs. k_0 (for $|E|\theta > 1$ and $E < 0$) for a monochromatic TM mode (blue). The interval within the red vertical dashed lines is the Klein zone. The intervals where $R = 1$ correspond to the mass gaps. The outer region, delimited by the orange vertical dashed lines is the propagation region. We also display the reflection coefficient for the TE modes (dashed green) as in Fig. 6. We have chosen $k_2 = 0.25$, $k_\perp = 0.5$, $E = -8$ in length units of $\sqrt{\theta}$

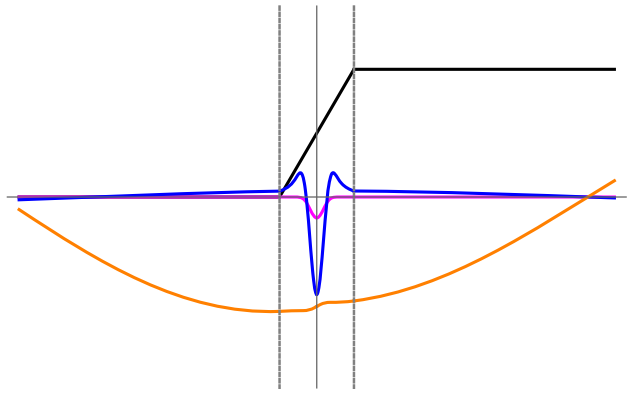

Fig. 11 Gauge field components a_0 (magenta), a_1 (blue) and a_P (orange) after removing the singular gauge transformation for the same parameters as in Fig. 9. To display all components in the same figure, a_0 (magenta) has been amplified and a_1 (blue) reduced by a factor 10

and permits to match the solutions (6.7) and (6.8) to determine the relation between the constants a, b, c, d. For this reason, the result expressed in (6.19) and (6.20) still holds in the Klein zone.

Note that, as for the TE modes, $R < 1$ even in the Klein zone. Of course, for a monochromatic wave with positive group velocity at $x^1 > L$, one takes $c = 0$ and $d = 1$ in (6.7)–(6.8), the reflection coefficient results $1/|r_L|^2$ and is thus greater than 1.

As for TE modes, this is interpreted as the result of photon production: the wave is totally reflected but a flux of photons created at the step runs in both directions.

Finally, one can also evaluate for TM modes the Klein paradox in the sense of a non-vanishing transmitted wave even for an infinitely high step. As for the TE modes, this does not occur for TM modes either. Using the standard asymp-

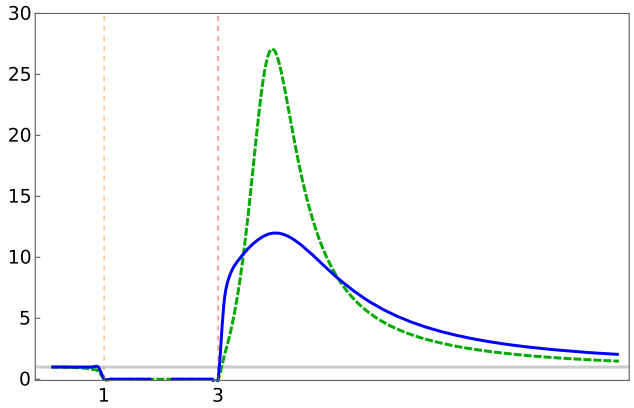

Fig. 12 T vs. $|E|$ for a wave packet of TM modes (blue). At the left of the orange dashed line, the propagation zone; at the right of the red dashed line, the Klein zone. We also display T for TE modes (dashed green) as in Fig. 7. We have chosen $E < 0$, $k_2 = 0.25$, $k_\perp = 0.5$, $k_0 = 1$ in length units of $\sqrt{\theta}$

totic behavior of confluent hypergeometric functions [48] one obtains the transmission coefficient for a wave packet for large values of the background electric field,[4]

$$T = \frac{|t_L|^2}{|r_L|^2} \sim \frac{2\pi\, k_0^2}{[\Gamma(\frac{3}{4})]^2\, k^1\, \sqrt{|E|}}. \tag{7.1}$$

Figure 12 shows T as a function of E.

8 Edge states

For very intense electric fields such that $\theta|E| < |k_\perp|/|k^2|$ a Klein zone is created between the left- and the right-mass gaps. Propagation with energies within this zone has been discussed in the previous sections.

On the contrary, for $\theta|E| < |k_\perp|/|k^2|$ there is an overlapping between both mass gaps. If the energy lies within this overlapping then both k^1 and κ^1 are purely imaginary, so it could be possible to find waves localized in the vicinity of the interface $x^1 = 0$ (edge states). Of course, for this to happen the solution must be appropriately matched all along the x^1 axis.

Propagation of TE modes is described by the Klein–Gordon equation with a step-like electrostatic potential that generates an homogeneous electric field in a region of width $2L$, so states localized in the x^1-direction are not to be expected.

As regards the TM modes, inspection of (6.5) shows that, apart from the same step-like potential, the field is subject to extra terms which depend on the incident energy k_0. One of these terms includes a delta-function with a negative coefficient so the equation could admit, a priori, bounded solutions.

To obtain bound states in the x^1-direction we look for solutions (6.7) and (6.8) with k^1 and κ^1 in the negative imaginary semi-axis,

$$k^1 = -i\sqrt{k_\perp^2 - k_0^2}, \tag{8.1}$$

$$\kappa^1 = -i\sqrt{k_\perp^2 - (k_0 + 2EL)^2}, \tag{8.2}$$

such that $b = c = 0$ to match the appropriate behavior at $x^1 \to \pm\infty$. This condition can only be implemented if the S-matrix is singular. In conclusion, the equation $\det S = 0$ determines the energies at which edge states could occur. Figure 13 shows that for some values of the parameters $E, \theta, k^2, k_\perp$ there is a finite number of edge states.

9 A magnetic background

As a complement of our results we give in this section a qualitative discussion of the fluctuations of a static homogeneous magnetic field which is localized at one side of a flat interface. We consider the noncommutative generalization of $\mathbb{R}^{3+1}$ but, as before, we choose coordinates such that $[\hat{x}^1, \hat{x}^2] = 2i\theta$ and $\hat{x}^3$ commutes with both $\hat{x}^1$ and $\hat{x}^2$. We assume that in the region $\hat{x}^1 > 0$ there exists a static homogeneous magnetic field with intensity B and directed along a unit vector $\check{t}_B$, tangent to the interface $\hat{x}^1 = 0$ or, equivalently, orthogonal to $\check{\imath}$, the unit vector in the x^1-direction.

The external current J^μ is supported at $\hat{x}^1 = 0$ and directed along the unit vector $\check{t}_J = \check{\imath} \times \check{t}_B$. For any given solution for the gauge field perturbations $a_\mu = (a_0, \vec{a})$, conditions (2.15) act as an obstruction to the choice of the temporal gauge; still, we can impose the axial gauge condition $\vec{a}_J = \vec{a} \cdot \check{t}_J = 0$. In this gauge the field, if written as $a_\mu(x^1)\, e^{-ik_0x^0 - ik_2x^2 - ik_3x^3}$, can be decomposed as

$$a_\mu(x^1) = a_T\,(k_B, k_0\,\check{t}_B) + a_L\,(k_0, k_B\,\check{t}_B) + a_1(x^1)\,\check{\imath}. \tag{9.1}$$

In this expression $k_B = \vec{k} \cdot \check{t}_B$, where $\vec{k} = (k_2, k_3)$. Note that the three terms in the decomposition are mutually orthogonal with respect to the Minkowski metric.

In this basis the component $a_T(x^1)$ decouples and one gets

$$-a_T'' + [-k_0^2 + (k_2 - \delta A_2)^2 + k_3^2]\, a_T = 0. \tag{9.2}$$

This equation is to be compared with (3.6) for the TE mode in the case of an electric background. In the asymptotic regions $|x^1| > L = |\theta k_2|$, where δA_2 is constant, the dispersion relation for a plane wave of momentum k^μ reads (see, e.g., [49])

[4] For large $|E|$ the transmission coefficient oscillates around this expression. For simplicity, we omit the oscillatory behavior.

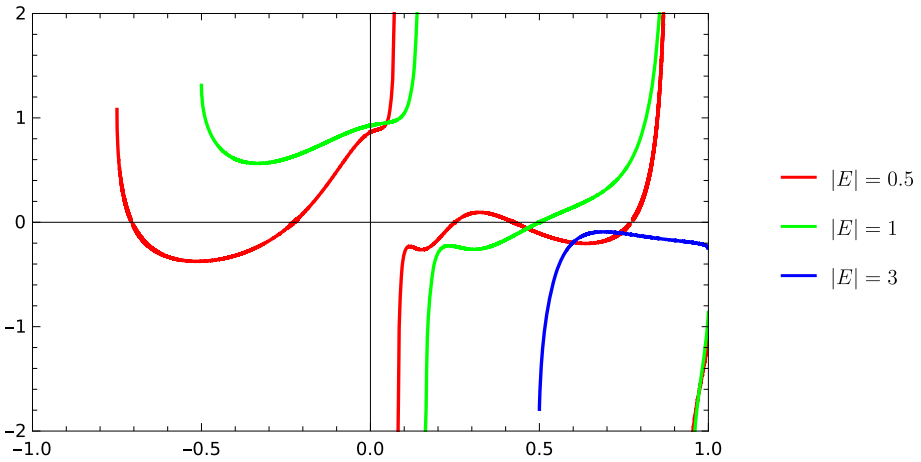

Fig. 13 The figure shows det S as a function of k_0 for different values of the electric field ($E < 0$). Each curve is defined in the interval $-2EL - k_P < k_0 < k_P$, which corresponds to the overlapping of the mass gaps. The transverse momenta were chosen as $k_2 = 0.25$, $k_P = 1$ (in units of $\sqrt{\theta}$.) Each intersection with the horizontal axis gives the energy of an edge state. The number of edge states decreases with increasing $|E|$

$$k_0^2 = k_1^2 + (k_2 - \delta A_2)^2 + k_3^2. \tag{9.3}$$

A wave propagates as long as its energy k_0 does not fall within the mass gaps in the regions $x^1 \to \pm\infty$. Since both gaps are centered at the origin, there is no Klein region and, as a consequence, no photon production; the field perturbation suffers an ordinary scattering ($R + T = 1$). However, for strong enough magnetic backgrounds, the gap at $x^1 > L$ might be wider than the one at $x^1 < -L$. In that case, low-energy photons get totally reflected at the magnetic step ($R = 1$). This is the expected behavior for a charged spinless particle scattered by an homogeneous magnetic field confined within parallel planes, which is the system described by (9.2).

Components a_1, a_L remain coupled but they satisfy relations completely analogous to (6.3), (6.4) and (6.5), with the obvious interchanges in the subindices corresponding to the x^0- and x^2-directions. As a consequence, the dispersion relation in the asymptotic regions is again dictated by (9.3). Therefore, the scattering of this polarization is qualitatively similar to the one already described for a_T: ordinary scattering ($R + T = 1$), total reflection for strong magnetic fields, and no photon production. The specific form of the reflection and transmission coefficients are expected to differ between both polarizations because, as for the electric background, they satisfy different equations at $|x^1| < L$.

10 Conclusions

Electromagnetism in Moyal space is a self-interacting theory, so perturbations of a classical configuration do not propagate freely but interact with the underlying background. Since this interaction does not show up for homogeneous backgrounds, we have considered two half-spaces separated by a flat interface: one half is free from background fields, the other is filled up with an homogeneous electric field. One each side a photon beam propagates free from interactions but suffers scattering at the interface. In this article we have determined the stationary states, both for TE and TM modes.

Each gauge field component which is perpendicular to the plane of incidence (TE mode) decouples and propagates as a massive, charged scalar particle. The mass is given by the momentum component parallel to the interface. Since the gauge field belongs to the adjoint representation of the $\star$-product, each TE mode only interacts with a homogeneous electric field restricted to a narrow region around the interface. As a consequence, TE modes reproduce the dynamics of a relativistic scalar field interacting with a step-like electrostatic field: $R < 1$ for a monochromatic wave (but $R > 1$ for a wave packet in the Klein regime) and, due to the finite width of the potential, super-Klein tunneling is suppressed and the transmission coefficients vanishes as the step height tends to infinity.

To solve for TM modes one needs to choose a particular gauge. We take the temporal gauge and solve the equations of motion. The reflection coefficient is computed and compared to the result for TE modes (Fig. 10). Also in this case, $R < 1$ for a monochromatic wave (as for scalar fields; unlike fermionic fields). In the Klein regime the wave interacts with a singularity, which is an artifact of the gauge choice. A careful analysis allows one to determine the appropriate matching conditions across the singularity. After removing the singularity with a gauge transformation, we determine the profiles of the propagating gauge fields.

As the electric field goes to infinity, the transmission coefficient also vanishes. The asymptotic behavior of T for TE and TM modes obeys the same power law but with a different coefficient ((5.20) and (7.1)).

For moderate electric fields, such that there is no separation between the left- and right-mass gaps, it might be possible that the electric field supports waves localized in the vicinity of the interface. Of course, this could only be the case for TM modes, for which the one-dimensional equation (6.5) contains a delta-function with a negative coefficient.

Figure 13 shows that for some values of the electric field a finite number of edge states may appear.

It is important to point out that the conserved current computed in this article – both for TE and TM modes – can be obtained from the asymptotic behavior of the canonical energy-momentum tensor $T_{\mu\nu} = -\frac{1}{2}\{F_{\mu\rho}, \partial_\nu A^\rho\}_\star + \frac{1}{4}\eta_{\mu\nu}F_\star^2$ (see [50]). As in ordinary Yang–Mills theories the construction of symmetric, traceless, gauge covariant or (covariantly) conserved energy-momentum tensors in NC gauge theories has been thoroughly studied [50–52]. Nevertheless, the conserved current considered in the present article is only used to illustrate the asymptotic behavior of the gauge fields profiles; our main purpose is to present the classical solutions which can be subsequently used to expand the quantized gauge field.

Before concluding we would like to put our results in a broader context. Let us first mention that although we have performed an analysis of the explicit solutions on top of a specific background $A_0(x^1)$, the conclusions of the preceding paragraphs can be applied to more general profiles. For instance, by analyzing the equations of motion satisfied by small perturbations of an arbitrary background $A_0(x^1)$ we have shown that the residual symmetry admits the temporal gauge. This choice allows the decoupling of TE and TM modes, whose dynamics is governed by Eqs. (3.6) and (6.5), respectively. Through these equations and according to the analysis followed in Sect. 4, one concludes that if the electric field takes constant asymptotic values $E_\pm$ at $x^1 \to \pm\infty$ then a Klein zone is produced if and only if $|(E_+ - E_-)\,\theta\cos\beta| > 1$. Therefore, as long as one maintains the asymptotic behavior of the background, the precise details of the electric field in the vicinity of the interface do not alter some qualitative aspects of the solutions, such as the generation of a Klein zone.

On the other hand, the specific behavior of the background in the vicinity of the interface can be analyzed along the lines of Sect. 8 in order to determine the existence of edge states for both types of polarizations. In fact, for appropriate $\delta A_0(x^1)$ both (3.6) and (6.5) might admit bound states. Of course, $|(E_+ - E_-)\,\theta\cos\beta| < 1$ arises as a necessary condition, i.e., edge states and photon production cannot occur simultaneously. This analysis holds for a general electric background but perpendicular to the interface.

On the contrary, cases in which the electric field has components which are tangent to the interface are much more difficult to approach because a nontrivial dependence on two coordinates becomes strongly intertwined through the Moyal product and separability gets spoiled. Nevertheless, note that whenever a surface separates a region with no electric field from a region with nonvanishing electric field $\vec{E}$ (as long as this field is generated uniquely by the electrostatic potential A_0) then $\vec{E}$ at the surface is normal.

A similar conclusion applies to the case of the magnetic background considered in Sect. 9: a homogeneous magnetic field tangent to the interface can be seen as an approximation in the neighborhood of a surface carrying a stationary current. As already mentioned, the solutions for the magnetic background can be readily obtained from the results of the electric background. The equations are completely analogous, their physical interpretation, of course, is qualitatively different.

This article therefore provides the spectrum of fluctuations around a specific background. In particular, fluctuation modes with energies in the Klein zone would indicate that inhomogeneities in a background electric field are capable of generating photon beams. We think that an expansion of the quantum field in the stationary modes described in this article would provide the rate of photon creation. In the S-matrix formalism, this is usually connected with the integral of the transmission coefficient – as a function of the incident energy – in the Klein region. On the other hand, the spectral decomposition of the operator of quantum fluctuations can also be used to compute the heat-trace, from which the imaginary part of the effective action (and, thus, the stability of the vacuum) can be studied. It would be interesting to compare the results with the already studied heat-kernel methods for NC theories [53–55]. Work along these two lines of research is currently under consideration.

Acknowledgements We thank Sergio Santa María Linárez for his participation in the early stages of this project, and Nicolás Grandi for useful discussions throughout this project. We also thank Fiorella Sol Beck and Maximiliano Ferro for reading the manuscript. The authors thank support from UNLP (through projects X909 and X931) and CONICET.

Data availability This manuscript has no associated data. [Author's comment: Data sharing not applicable to this article as no datasets were generated or analysed during the current study].

Funded by SCOAP[3].

References

1. M.R. Douglas, N.A. Nekrasov, Noncommutative field theory. Rev. Mod. Phys. **73**, 977–1029 (2001). arXiv:hep-th/0106048
2. R.J. Szabo, Quantum field theory on noncommutative spaces. Phys. Rep. **378**, 207–299 (2003). arXiv:hep-th/0109162

3. P. Vitale, M. Adamo, R. Dekhil, D. Fernández-Silvestre, Introduction to noncommutative field and gauge theory. arXiv:2309.17369
4. N. Chair, M.M. Sheikh-Jabbari, Pair production by a constant external field in noncommutative QED. Phys. Lett. B **504**, 141–146 (2001). arXiv:hep-th/0009037
5. A.I. Nikishov, On the theory of scalar pair production by a potential barrier. arXiv:hep-th/0111137
6. S.P. Gavrilov, D.M. Gitman, Quantization of charged fields in the presence of critical potential steps. Phys. Rev. D **93**(4), 045002 (2016). arXiv:1506.01156
7. D.V. Vassilevich, Heat kernel expansion: user's manual. Phys. Rep. **388**, 279–360 (2003). arXiv:hep-th/0306138
8. G.C. Nayak, P. van Nieuwenhuizen, Soft-gluon production due to a gluon loop in a constant chromo-electric background field. Phys. Rev. D **71**, 125001 (2005). arXiv:hep-ph/0504070
9. A. Ilderton, J. Lundin, M. Marklund, Strong field, noncommutative QED. SIGMA **6**, 041 (2010). arXiv:1003.4184
10. R. Fresneda, D.M. Gitman, A.E. Shabad, Photon propagation in noncommutative QED with constant external field. Phys. Rev. D **91**(8), 085005 (2015). arXiv:1501.04987
11. D.V. Vassilevich, A. Yurov, Space-time noncommutativity tends to create bound states. Phys. Rev. D **69**, 105006 (2004). arXiv:hep-th/0311214
12. Rolf G. Winter, Klein paradox for the Klein–Gordon equation. Am. J. Phys. **27**, 355 (1959)
13. A. Calogeracos, N. Dombey, Klein tunneling and the Klein paradox. Int. J. Mod. Phys. A **14**, 631–644 (1999). arXiv:quant-ph/9806052
14. K. Kim, Super-Klein tunneling of Klein–Gordon particles. Results Phys. **12**, 1391–1394 (2019)
15. O. Klein, Die Reflexion von Elektronen an einem Potentialsprung nach der relativistischen Dynamik von Dirac. Z. Phys. **53**, 157 (1929)
16. A.I. Nikishov, Barrier scattering in field theory removal of Klein paradox. Nucl. Phys. B **21**, 346–358 (1970)
17. A. Hansen, F. Ravndal, Klein's paradox and its resolution. Phys. Scr. **23**, 1036 (1981)
18. C.A. Manogue, The Klein paradox and superradiance. Ann. Phys. **181**, 261 (1988)
19. N. Dombey, A. Calogeracos, Seventy years of the Klein paradox. Phys. Rep. **315**, 41–58 (1999)
20. A. Chervyakov, H. Kleinert, On electron-positron pair production by a spatially inhomogeneous electric field. Phys. Part. Nucl. **49**(3), 374–396 (2018). arXiv:1112.4120
21. S. Evans, J. Rafelski, Particle production at a finite potential step: transition from Euler–Heisenberg to Klein paradox. Eur. Phys. J. A **57**(12), 341 (2021). arXiv:2108.12959
22. P. Krekora, Q. Su, R. Grobe, Klein paradox in spatial and temporal resolution. Phys. Rev. Lett. **92**, 040406 (2004)
23. T. Cheng, Q. Su, R. Grobe, Introductory review on quantum field theory with space-time resolution. Contemp. Phys. **51**(4), 315–330 (2010)
24. Q.Z. Lv, S. Dong, Y.T. Li, Z.M. Sheng, Q. Su, R. Grobe, Role of the spatial inhomogeneity on the laser-induced vacuum decay. Phys. Rev. A **97**(2), 022515 (2018)
25. M. Alkhateeb, A. Matzkin, Space-time-resolved quantum field approach to Klein-tunneling dynamics across a finite barrier. Phys. Rev. A **106**(6), L060202 (2022). arXiv:2205.15119
26. F. Sauter, Über das Verhalten eines Elektrons im homogenen elektrischen Feld nach der relativistischen Theorie Diracs. Z. Phys. **69**, 742–746 (1931)
27. S.P. Gavrilov, D.M. Gitman, Scattering and pair creation by a constant electric field between two capacitor plates. Phys. Rev. D **93**(4), 045033 (2016). arXiv:1511.02915
28. S. Minwalla, M. Van Raamsdonk, N. Seiberg, Noncommutative perturbative dynamics. JHEP **02**, 020 (2000). arXiv:hep-th/9912072
29. I.Y. Aref'eva, D.M. Belov, A.S. Koshelev, Two loop diagrams in noncommutative phi**4(4) theory. Phys. Lett. B **476**, 431–436 (2000). arXiv:hep-th/9912075
30. M. Hayakawa, Perturbative analysis on infrared and ultraviolet aspects of noncommutative QED on R**4. arXiv:hep-th/9912167
31. M. Chaichian, M.M. Sheikh-Jabbari, A. Tureanu, Hydrogen atom spectrum and the Lamb shift in noncommutative QED. Phys. Rev. Lett. **86**, 2716 (2001). arXiv:hep-th/0010175
32. V.P. Nair, A.P. Polychronakos, Quantum mechanics on the noncommutative plane and sphere. Phys. Lett. B **505**, 267–274 (2001). arXiv:hep-th/0011172
33. J. Gamboa, M. Loewe, F. Mendez, J.C. Rojas, The Landau problem and noncommutative quantum mechanics. Mod. Phys. Lett. A **16**, 2075–2078 (2001). arXiv:hep-th/0104224
34. P.A. Horvathy, The noncommutative Landau problem and the Peierls substitution. Ann. Phys. **299**, 128–140 (2002). arXiv:hep-th/0201007
35. H. Falomir, P. Pisani, F. Vega, D. Cárcamo, F. Méndez, M. Loewe, On the algebraic structure of rotationally invariant two-dimensional Hamiltonians on the noncommutative phase space. J. Phys. A **49**(5), 055202 (2016). arXiv:1507.06932
36. H. Falomir, J. Liniado, P. Pisani, Algebraic structure of Dirac Hamiltonians in non-commutative phase space. J. Phys. A **55**(46), 465202 (2022). arXiv:2205.00898
37. M. Chaichian, A. Demichev, P. Presnajder, M.M. Sheikh-Jabbari, A. Tureanu, Aharonov–Bohm effect in noncommutative spaces. Phys. Lett. B **527**, 149–154 (2002). arXiv:hep-th/0012175
38. H. Falomir, J. Gamboa, M. Loewe, F. Mendez, J.C. Rojas, Testing spatial noncommutativity via the Aharonov–Bohm effect. Phys. Rev. D **66**, 045018 (2002). arXiv:hep-th/0203260
39. A. Kokado, T. Okamura, T. Saito, Noncommutative quantum mechanics and Seiberg–Witten map. Phys. Rev. D **69**, 125007 (2004). arXiv:hep-th/0401180
40. K. Li, S. Dulat, The Aharonov–Bohm effect in noncommutative quantum mechanics. Eur. Phys. J. C **46**, 825–828 (2006). arXiv:hep-th/0508193
41. B. Harms, O. Micu, Noncommutative quantum Hall effect and Aharonov–Bohm effect. J. Phys. A **40**, 10337–10348 (2007). arXiv:hep-th/0610081
42. M. Chaichian, M. Langvik, S. Sasaki, A. Tureanu, Gauge covariance of the Aharonov–Bohm phase in noncommutative quantum mechanics. Phys. Lett. B **666**, 199–204 (2008). arXiv:0804.3565
43. O.F. Dayi, A. Jellal, Hall effect in noncommutative coordinates. J. Math. Phys. **43**, 4592 (2002) [Erratum: J. Math. Phys. **45**, 827 (2004)]. arXiv:hep-th/0111267
44. K. Li, J. Wang, The topological AC effect on noncommutative phase space. Eur. Phys. J. C **50**, 1007–1011 (2007). arXiv:hep-th/0608100
45. M. Chaichian, S. Ghosh, M. Langvik, A. Tureanu, Dirac quantization condition for monopole in noncommutative space-time. Phys. Rev. D **79**, 125029 (2009). arXiv:0902.2453
46. J. Gomis, T. Mehen, Space-time noncommutative field theories and unitarity. Nucl. Phys. B **591**, 265–276 (2000). arXiv:hep-th/0005129
47. D. Bahns, S. Doplicher, K. Fredenhagen, G. Piacitelli, On the unitarity problem in space-time noncommutative theories. Phys. Lett. B **533**, 178–181 (2002). arXiv:hep-th/0201222
48. M. Abramowitz, I.A. Stegun (eds.), *Handbook of mathematical functions* (Dover Publications, Tenth Printing, 1972)
49. Z. Guralnik, R. Jackiw, S.Y. Pi, A.P. Polychronakos, Testing noncommutative QED, constructing noncommutative MHD. Phys. Lett. B **517**, 450–456 (2001). arXiv:hep-th/0106044

50. J.M. Grimstrup, B. Kloibock, L. Popp, V. Putz, M. Schweda, M. Wickenhauser, The Energy momentum tensor in noncommutative gauge field models. Int. J. Mod. Phys. A **19**, 5615–5624 (2004). arXiv:hep-th/0210288
51. A.K. Das, J. Frenkel, On the energy momentum tensor in noncommutative gauge theories. Phys. Rev. D **67**, 067701 (2003). arXiv:hep-th/0212122
52. H. Balasin, D.N. Blaschke, F. Gieres, M. Schweda, On the energy-momentum tensor in Moyal space. Eur. Phys. J. C **75**(6), 284 (2015). arXiv:1502.03765
53. D.V. Vassilevich, Noncommutative heat kernel. Lett. Math. Phys. **67**, 185–194 (2004). arXiv:hep-th/0310144
54. R. Bonezzi, O. Corradini, S.A. Franchino Viñas, P. Pisani, Worldline approach to noncommutative field theory. J. Phys. A **45**, 405401 (2012). arXiv:1204.1013
55. N. Ahmadiniaz, O. Corradini, D. D'Ascanio, S. Estrada-Jiménez, P. Pisani, Noncommutative U(1) gauge theory from a worldline perspective. JHEP **11**, 069 (2015). arXiv:1507.07033